Chemistry of Metals and Alloys

Chem. Met. Alloys 11 (2018) 77-84
Ivan Franko National University of Lviv
www.chemetal-journal.org

Effect of phase composition of Ti–Zr–Mn–V alloys on the hydrogen sorption properties

V. DEKHTYARENKO[1]*, T. PRYADKO[1], O. BOSHKO[2]

[1] *Laboratory of Eutectic Alloys, G.V. Kurdyumov Institute for Metal Physics of NASU, Akad. Vernadsky Ave. 36, 03142 Kyiv, Ukraine*
[2] *Department of Crystallization, G.V. Kurdyumov Institute for Metal Physics of NASU, Akad. Vernadsky Ave. 36, 03142 Kyiv, Ukraine*
* *Corresponding author. Tel. +380-44-4241220; e-mail: devova@i.ua*

Received May 5, 2018; accepted December 26, 2018; available on-line March 29, 2019

The phase composition and crystal structures of heterophase Ti–Zr–Mn–V alloys were studied by scanning electron microscopy and X-ray diffraction. The structure of the as-cast and annealed alloys consisted of a Laves phase and a *bcc* solid solution. It is shown that the alloys interact with hydrogen at room temperature and a pressure of 0.23 MPa with an incubation period of 6-10 min and a duration of the absorption process of 10 min. The resulting hydrogen sorption capacity was more than 2 wt.%. Additional processing of the obtained hydrides could increase the hydrogen sorption capacity.

Hydrogen storage / Heterophase alloy / Hydrides / Sieverts' method / Hydrogenation

1. Introduction

Numerous investigations aim at creating materials with given properties, such as temperature and pressure of synthesis and decomposition of their hydrides, to solve specific technical problems of hydrogen energetics [1]. Up to now, the most used materials have been $LaNi_5$ and alloys based on it. However, the weight of this class of materials limits their use in mobile energy sources.

As of today, the most serious candidates for use as hydrogen batteries / accumulators are intermetallics of the AB_2 type, such as $TiMn_2$. These compounds have acceptable kinetic parameters of the sorption / desorption processes and high sorption capacities H/*Me* ~ 1.0 [2,3]. In addition, they have relatively low weight and low cost, which is especially important for car batteries. To increase the sorption capacity and improve the hydrogenation kinetics, several authors [4-8] have proposed to partially replace titanium by zirconium in the Ti–Mn alloys, since zirconium has higher compatibility with hydrogen than titanium.

Ivanchenko *et al.* [9] significantly increased the concentration limit of the homogeneity range of the AB_2 intermetallic in the Ti–Zr–Mn system, thanks to an optimal ratio of titanium and zirconium. They managed to increase the sorption capacity of a $Ti_{0.154}Zr_{0.302}Mn_{0.544}$ alloy to H/*Me* ≈ 1.41 and improve the kinetic parameters of the hydrogen sorption and desorption processes. However, the higher zirconium content raised the desorption temperature to 550°C [10].

An important feature of the Laves phase in the Ti–Zr–Mn system is an exceptionally wide (for this class of intermetallics) homogeneity range (~10 at.%), characterized by a number of stable non-stoichiometric compositions with significant deviations from stoichiometry [11]. The introduction of vanadium into alloys of the Ti–Zr–Mn system makes it possible to further expand the region of existence of the Laves phase [12].

According to a crystal chemical analysis [13], the structure of the C14 hexagonal Laves phase has seven interstitial sites available for hydrogen atoms. However, a study of non-stoichiometric alloys of the Ti–Mn–V and Ti–Zr–Mn–V systems [14] has shown that in this case, differently from stoichiometric AB_2 alloys, the formation of a higher amount of interstitial sites suitable for hydrogen storage is possible. This is due to the fact that in non-stoichiometric alloys the sites of the manganese atoms are partially occupied by titanium atoms. In addition, vanadium, another hydride-forming metal, acts as *B*-component and a possibility to fill additional interstitial sites with hydrogen atoms emerges, thanks to the increase of the ratio of hydrogen-active *B*-components. An analysis of the interaction of the alloys with hydrogen made it possible to obtain materials able to store up to 2 wt.% hydrogen [15].

Investigating the kinetic and sorption parameters of hydrogenation of AB_2-type intermetallics, Pickering *et al.* [16] found that the best kinetic and sorption parameters were observed for alloys in which the Laves phase coexists with a *bcc* solid solution that exhibits similar reaction kinetics and practically identical stability of the hydride. A new concept for the production of high hydrogen capacity alloys, called "Laves phase-related *bcc* solid solution", was proposed. According to Huang *et al.* [17], alloying of these alloys with vanadium leads to an increase of the volume fraction of the *bcc* solid solution and, as a consequence, to an increase of the hydrogen capacity.

Considering this concept as promising for the creation of alloys for safe transportation and storage of hydrogen in the bound state, we decided to study the hydrogen sorption characteristics of heterophase alloys of the Ti–Zr–Mn–V system with Laves phase-related *bcc* solid solution.

2. Materials studied and experimental details

Compositions of heterophase composites with a certain ratio of *A* and *B* components were selected according to the phase diagram [18,19], in such a way that a *bcc* solid solution should coexist with the Laves phase. Two compositions were chosen: $Ti_{19.8}Zr_{34.8}Mn_{43.3}V_{2.1}$ and $Ti_{32.1}Zr_{18.9}Mn_{42.0}V_{7.0}$ (see Table 1).

Alloy ingots of up to 30 g were melted (six-time remelting) in a laboratory arc furnace with a non-consumable tungsten electrode and a cooled copper hearth in purified argon atmosphere, using iodide titanium (of 99.95% purity), iodide zirconium (99.975%), as well as electrolytic vanadium (99.9%) and manganese (of 99.9%), as starting materials. The deviation of the composition of the alloys from the nominal composition was determined by fluorescence X-ray spectroscopy (VRA-30). Match with the nominal composition was within the experimental error (±0.03%).

The study was performed on as-cast and annealed samples. Annealing was carried out in a SNVL-1.3.1/16M2 furnace for 30 h in a vacuum of 10^{-3} Pa with a heating rate of 20°C/min. Isothermal annealing at 900°C was chosen to provide maximum diffusion of the components, while preventing melting.

The phase composition and the crystal lattice parameters were determined by X-ray diffraction (XRD), using a DRON-3M diffractometer with a standard GUR-8 goniometer. Scanning was performed using Co *Kα* radiation. The X-ray diffraction peaks were indexed using the database of the International Centre for Diffraction Data (JCPDS).

Metallographic research was carried out using an optical microscope "Neophot-32" with a magnification of up to 2000×. The volume fractions of the different phases and grain areas were analyzed using Maud and ImageJ programs. SEM images and element distribution maps were obtained with a VEGA3 TESCAN microscope operating at 20 kV, equipped with an energy-dispersive X-ray spectroscopy (EDX) facility.

The interaction of the alloys with hydrogen at room temperature and a pressure of ~0.23 MPa was studied by Sieverts' method, using IVGM-2M equipment [20]. Sorption-purified hydrogen was introduced into the vacuumized ($1.33 \cdot 10^{-3}$ Pa) reaction chamber at room temperature. The amount of absorbed hydrogen was determined by weighing with an accuracy of $1.5 \cdot 10^{-5}$ g and changing the pressure in a closed reaction volume. Studies on hydrogen desorption were carried out on an automated dilatometric complex (ADC) with a mass spectrometer unit [21].

3. Results and discussion

3.1 Structure and phase composition of the alloys

As expected, the structures of the $Ti_{19.8}Zr_{34.8}Mn_{43.3}V_{2.1}$ and $Ti_{32.1}Zr_{18.9}Mn_{42.0}V_{7.0}$ alloys consisted of large crystals of the λ Laves phase and β *bcc* solid solution (Fig. 1). A study of the evolution of the microstructure and phase composition of the alloys during the heat treatment showed that annealing in a vacuum of 10^{-3} Pa and a temperature of 900°C led to coagulation of the phase constituents. When the duration of the isothermal annealing was increased, growth of the phase constituents was observed as a result of crystalline coarsening, leading to the formation of more or less large phase aggregates.

Using the ImageJ software, it was found that, after annealing, the grain area of the intermetallic had increased from 450…1500 to 1000…3000 μm^2, and, that of the β-solid solution from 70…150 to 400…1000 μm^2. The specific surface of the interphase boundaries decreased by a factor of approximately 5. In addition, the volume ratio of the λ Laves phase and β *bcc* phase (Sλ / Sβ) changed during annealing, as a result of the redistribution of the components:

Table 1 Nominal compositions of the alloys.

Alloy	Chemical elements							
	at.%				wt.%			
	Ti	Zr	Mn	V	Ti	Zr	Mn	V
1	19.8	34.8	43.3	2.1	14.34	48.04	36.00	1.62
2	32.1	18.9	42.0	7.0	25.94	29.10	38.94	6.02

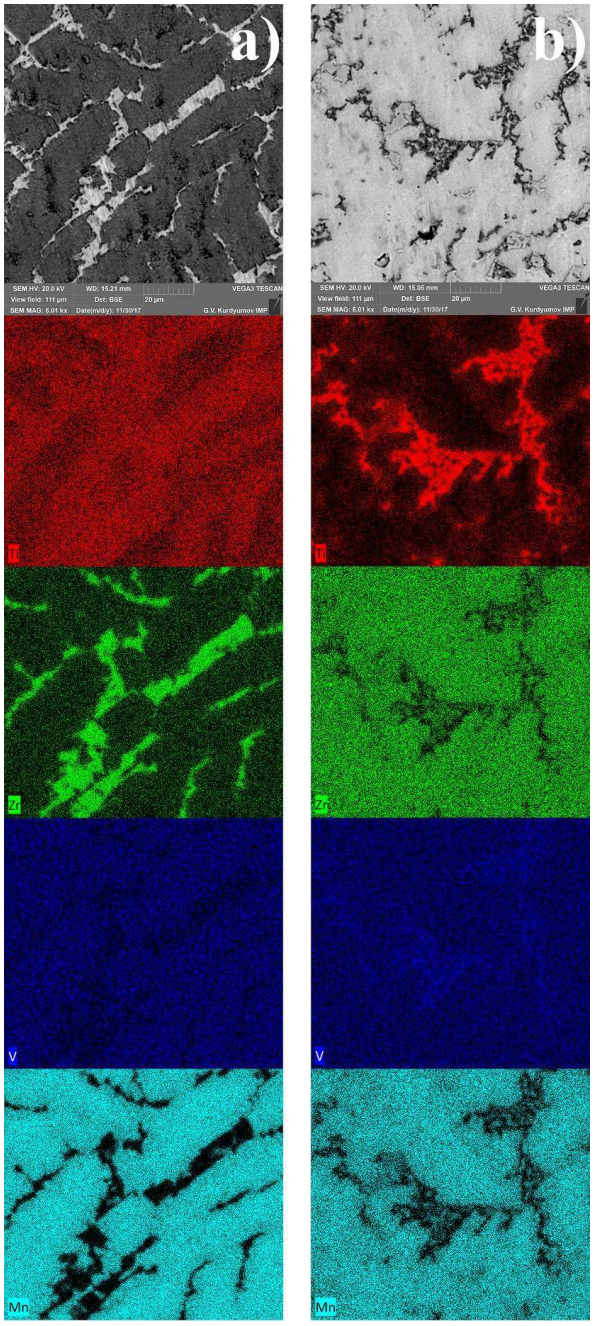

Fig. 1 Microstructure and element distribution maps of $Ti_{19.8}Zr_{34.8}Mn_{43.3}V_{2.1}$ (a), and $Ti_{32.1}Zr_{18.9}Mn_{42.0}V_{7.0}$ (b) as-cast samples.

from 75.06% / 24.94% to 72.16% / 27.84% for the $Ti_{19.8}Zr_{34.8}Mn_{43.3}V_{2.1}$ alloy and from 79.97% / 20.03% to 76.76% / 23.24% for the $Ti_{32.1}Zr_{18.9}Mn_{42.0}V_{7.0}$ alloy. The same specimens were subjected to metallographic analysis before and after annealing, and the data were averaged over several sections of ingots.

The metallographic studies were confirmed by XRD analysis (Table 2). The following phases were detected in the X-ray diffraction patterns of the investigated alloys:

- Laves phase $(Ti,Zr)(Mn,V)_{2-x}$ with a hexagonal lattice (space group $P6_3/mmc$, Pearson symbol $hP12$, prototype $MgZn_2$);
- β-solid solution (Ti,Zr,Mn,V) with a cubic lattice (space group $Im\text{-}3m$, Pearson symbol $cI2$, prototype W).

The chemical compositions of the individual phases were determined by EDX and the ratio of coexisting phases was established from XRD of the annealed samples, using the software Maud (Table 3).

3.2. Hydrogenation

The sorption properties of the alloys were studied at room temperature and a hydrogen pressure of 0.23 MPa (Fig. 2). The incubation period for the $Ti_{19.8}Zr_{34.8}Mn_{43.3}V_{2.1}$ alloy was 10 min, and for the $Ti_{32.1}Zr_{18.9}Mn_{42.0}V_{7.0}$ alloy it was 6 min. The absorption process was in both cases completed within 10 min, while the concentration of absorbed hydrogen was 2.16 and 2.20 wt.%, respectively (Table 4). Comparing these data with the corresponding data for single-phase alloys with Laves phase structure [3,9], it can be argued that the presence of *bcc* solid solution in the phase composition does not worsen the kinetic parameters of the hydrogenation process, and leads to an increase of the hydrogen storage capacity. Further holding for another 2 h did not lead to an increase of the amount of absorbed hydrogen.

In the case of saturation by hydrogen, *i.e.* absorption by the alloy of the highest possible concentration, complete destruction of the sample into powder occurred because of the high flow rate of the process and the low hydrogenation temperature, and hence, insufficient time for the relaxation of stresses.

The XRD phase analysis revealed that the final product of the hydrogenation of both the cast and annealed alloys consisted of hydrides formed on the basis of the parent alloy phases (see Table 2):

- δ is a hydride $(Ti,Zr,V,Mn)H_{2-x}$ of CaF_2 type based on the solid solution of metals with *fcc* structure;
- λ is a hydride $(Ti,Zr)(V,Mn)_{2-x}H_{1+x}$ based on the Laves phase with $MgZn_2$-type crystal structure.

SEM images of the microstructures of the alloys are shown in Fig. 1. Our assumption that vanadium, which is a β-stabilizer for titanium alloys and forms an AB_2 Laves phase with zirconium, should be evenly distributed among the coexisting phases, and that vanadium should substitute for both the *A* and *B* components in the intermetallic Laves phase, was confirmed by the element distribution maps (see Fig. 1). These maps also indicate that the amount of manganese in the *bcc* solid solution is minimal, because of the significant deviation of the compositions of the intermetallics from stoichiometry. The base of the β-phase in the $Ti_{32.1}Zr_{18.9}Mn_{42.0}V_{7.0}$ alloy is titanium, while in $Ti_{19.8}Zr_{34.8}Mn_{43.3}V_{2.1}$ it is zirconium.

Table 2 Crystallographic data for the as-cast alloys and the products of hydrogenation.

Alloy	Crystal lattice parameters ± 0.0009, nm					
	As-cast		After hydrogenation at 0.23 MPa and 20°C		After applying additional conditions	
	λ-phase	β-phase	λ-phase	δ-phase	λ-phase	δ-phase
$Ti_{19.8}Zr_{34.8}Mn_{43.3}V_{2.1}$	*a* = 0.5169 *c* = 0.8492	*a* = 0.3365	*a* = 0.5597 *c* = 0.9193	*a* = 0.4471	*a* = 0.5627 *c* = 0.9242	*a* = 0.4508
$Ti_{32.1}Zr_{18.9}Mn_{42.0}V_{7.0}$	*a* = 0.5113 *c* = 0.8400	*a* = 0.3327	*a* = 0.5501 *c* = 0.9035	*a* = 0.4437	*a* = 0.5594 *c* = 0.9188	*a* = 0.4443

Table 3 Chemical composition (from EDX) and ratio of coexisting phases (from XRD) in the annealed alloys.

Alloy	Phase	Composition, at.% ± 0.03	λ/β phase ratio
$Ti_{19.8}Zr_{34.8}Mn_{43.3}V_{2.1}$	λ β	18.12Ti-24.37Zr-56.72Mn-2.33V 24.84Ti-66.07Zr-3.07Mn-1.41V	0.7499/0.2501
$Ti_{32.1}Zr_{18.9}Mn_{42.0}V_{7.0}$	λ β	11.18Ti-31.31Zr-51.55Mn-7.25V 46.79Ti-35.24Zr-4.06Mn-6.01V	0.7989/0.2011

Table 4 Kinetic parameters of the hydrogenation ($\tau_{inc.}$ – incubation time, $\tau_{hydro.}$ – hydrogen sorption time, C_H – hydrogen sorption capacity).

Alloy	Hydrogenation conditions		$\tau_{inc.}$, min	$\tau_{hydro.}$, min	C_H, wt.%
	T, °C	*p*, MPa			
$Ti_{19.8}Zr_{34.8}Mn_{43.3}V_{2.1}$	20	0.23	10	10	2.16
$Ti_{32.1}Zr_{18.9}Mn_{42.0}V_{7.0}$	20	0.23	6	10	2.20
Additional conditions					
$Ti_{19.8}Zr_{34.8}Mn_{43.3}V_{2.1}$	400	3		60	2.29
$Ti_{32.1}Zr_{18.9}Mn_{42.0}V_{7.0}$	400	3		60	2.33

The results suggest that phase decomposition does not occur during hydrogenation of the alloys. Saturation by hydrogen is accompanied by an isotropic increase of the volume of the unit cell of the Laves phase by 25-27%.

An attempt was made to increase the sorption capacity of the alloys by changing the temperature-pressure conditions. For this, the pressure of the hydrogen atmosphere surrounding the hydrides was raised to 2.0 MPa. The hydrogenation did not resume within 24 h. The next step was to heat the alloys to 400°C. The hydrogen capacity of the $Ti_{19.8}Zr_{34.8}Mn_{43.3}V_{2.1}$ and $Ti_{32.1}Zr_{18.9}Mn_{42.0}V_{7.0}$ alloys increased to 2.29 and 2.33 wt.%, respectively, after 1-h holding at this temperature.

In order to estimate the hydrogen storage capacity of the β-solid solution and the Laves phase separately, the molar parts of the two phases in the alloys was calculated by the Rietveld method (see Table 3). Since no phase decomposition occurred during hydrogen saturation, it can be assumed that the ratio of the molar parts of hydrides obtained on the basis of each phase is maintained equal to the ratio of molar parts in the initial state. The increase of the volume of the unit cell of the Laves phase per metal atom allowed evaluating the sorption capacity of the intermetallic, and the residual amount of absorbed hydrogen may be attributed to the δ-hydride (Fig. 3).

Active hydrogen absorption starts already at room temperature and surface activation takes place due to uncompensated interatomic bonds at the surface of the Laves phase. As a result, dissociation of hydrogen molecules is facilitated, causing rapid penetration into the intermetallic matrix, followed by hydrogen penetration along the interphase boundaries. At the same time, substantial increase of the volume of the unit cell of the intermetallic leads to pulverization and the formation of a surface cleaned from oxide film. This is true not only for the intermetallic, but also for the adjacent surfaces of the crystallites of the *bcc* solid solution, which gets involved in the process of hydrogenation. Although the solid solution does not reach its maximum sorption capacity even under the additional conditions applied here, the total amount of

hydrogen absorbed by the heterophase alloys exceeds the values reported for single-phase intermetallics (Fig. 4).

The increase of the hydrogen sorption capacity of the $Ti_{19.8}Zr_{34.8}Mn_{43.3}V_{2.1}$ and $Ti_{32.1}Zr_{18.9}Mn_{42.0}V_{7.0}$ alloys can be explained by the redistribution of hydrogen-active metal atoms in the tetrahedral voids, and by an increase of the proportion of hydride-forming components.

The hydrogen desorption of the hydrogenation products was studied after pumping out the reactor to a pressure of ~$2\cdot10^{-4}$ MPa. It was established that the process of dehydrogenation of the alloys starts at room temperature, but just a small amount of the absorbed hydrogen could be removed under these conditions. It was, however, possible to enhance the desorption process by heating, and to complete it when the temperature reached 450°C (Fig. 5).

Alloys subjected to sorption-desorption cycling have activated surfaces, and the samples were able to absorb hydrogen at room temperature and a pressure of 0.2 MPa from the first seconds of contact with the hydrogen medium. Although the sorption capacity remained unchanged, the time to achieve its maximum possible value was extremely reduced. This improvement of the kinetic parameters can be explained by the disintegration of the bulk samples into powders during the sorption-desorption cycle. An additional factor is the decrease of the concentration of oxygen on the surface of and inside the hydride particles, as a result of the interaction with atomic hydrogen. The kinetic parameters of the sorption and desorption processes and the hydrogen sorption capacity of the alloys hardly changed in subsequent cycles. The increase of the rate of hydrogen absorption is associated with an increase of the reactive surface area due to the smaller size of the particles.

Conclusions

A high hydrogenation rate was achieved thanks to the relaxation of stresses arising in the intermetallic crystals upon absorption of hydrogen that takes place during the destruction of the compact sample, and the formation of surfaces free from oxide barrier layer. The presence of a *bcc* solid solution does not affect the incubation period of the hydrogenation process, but leads to an increase of the hydrogen storage capacity.

The possibility to increase the sorption capacity of each phase and the alloy as a whole was proven by changing the temperature-pressure conditions.

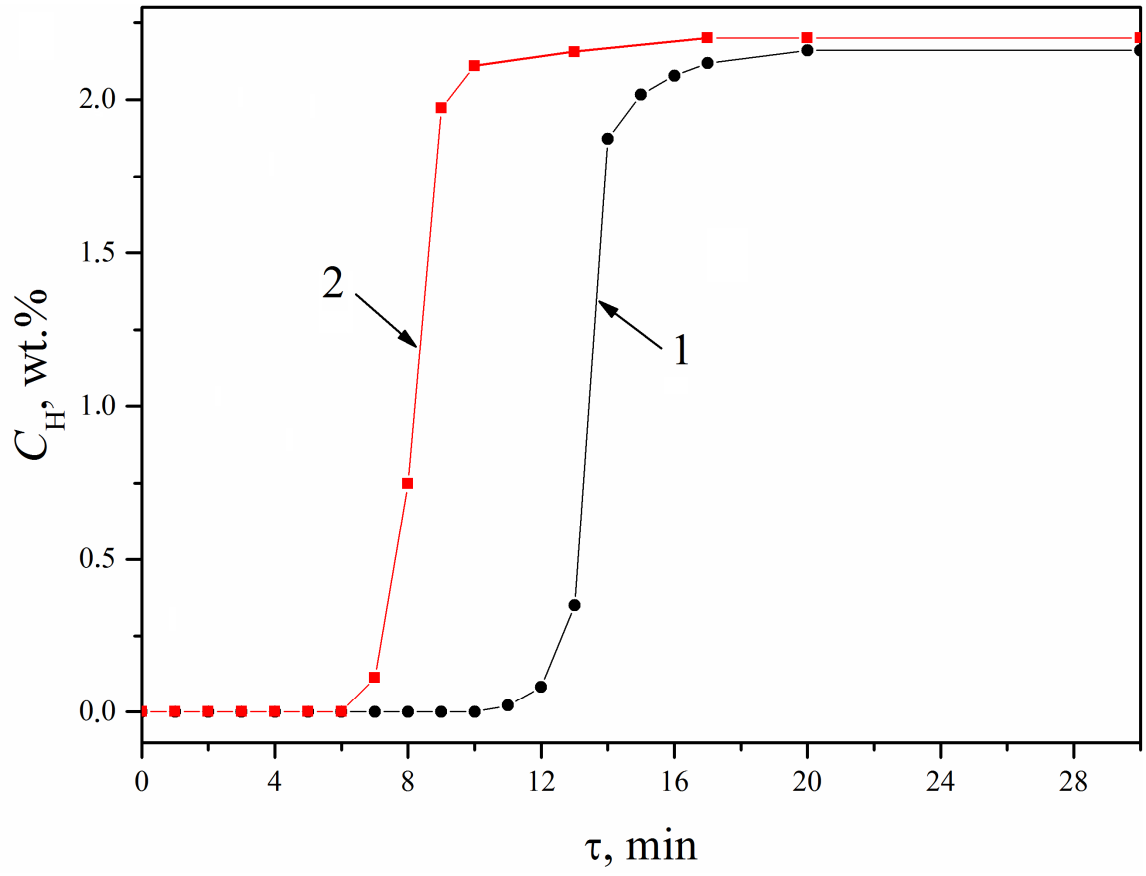

Fig. 2 Time dependency of the hydrogen concentration: 1 – $Ti_{19.8}Zr_{34.8}Mn_{43.3}V_{2.1}$, 2 – $Ti_{32.1}Zr_{18.9}Mn_{42.0}V_{7.0}$.

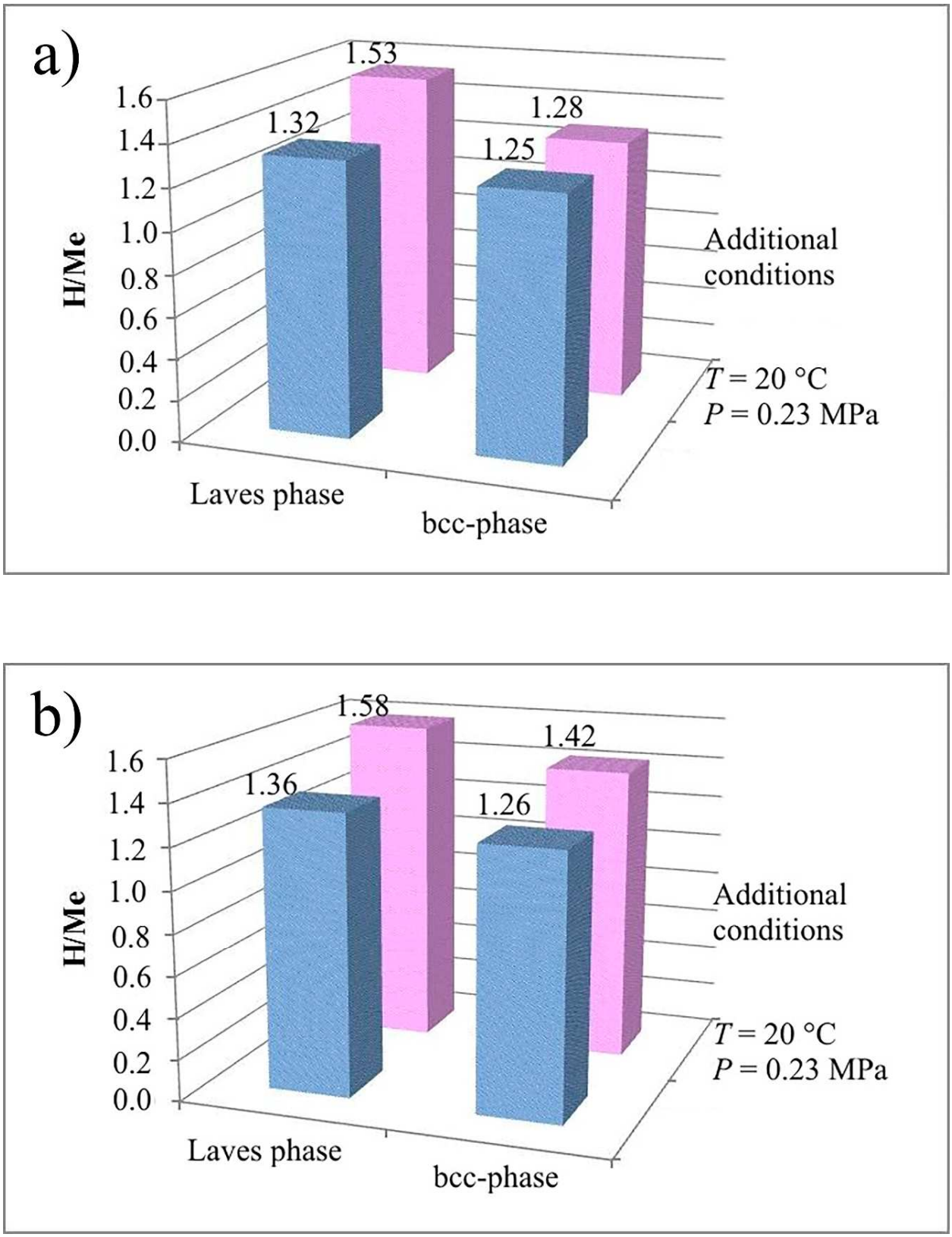

Fig. 3 Hydrogen sorption capacity of the individual phases in the $Ti_{19.8}Zr_{34.8}Mn_{43.3}V_{2.1}$ (a) and $Ti_{32.1}Zr_{18.9}Mn_{42.0}V_{7.0}$ (b) alloys during hydrogenation at room temperature, before (blue) and after (pink) applying additional conditions (p = 2.0 MPa, T = 400°C).

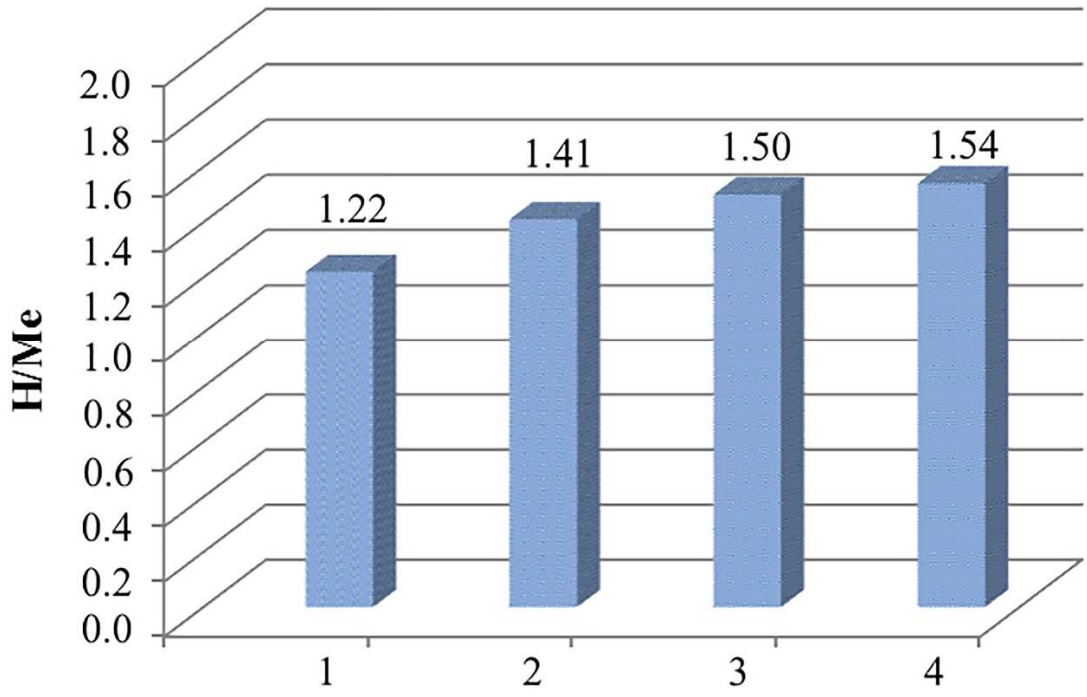

Fig. 4 Hydrogen sorption capacity of Laves phase intermetallics 1 – $(Ti_{0.34}Zr_{0.66})Mn_{1.4}$ [3], 2 – $(Ti_{0.34}Zr_{0.66})Mn_{1.2}$ [9] and heterophase alloys 3 – $Ti_{19.8}Zr_{34.8}Mn_{43.3}V_{2.1}$, 4 –$Ti_{32.1}Zr_{18.9}Mn_{42.0}V_{7.0}$.

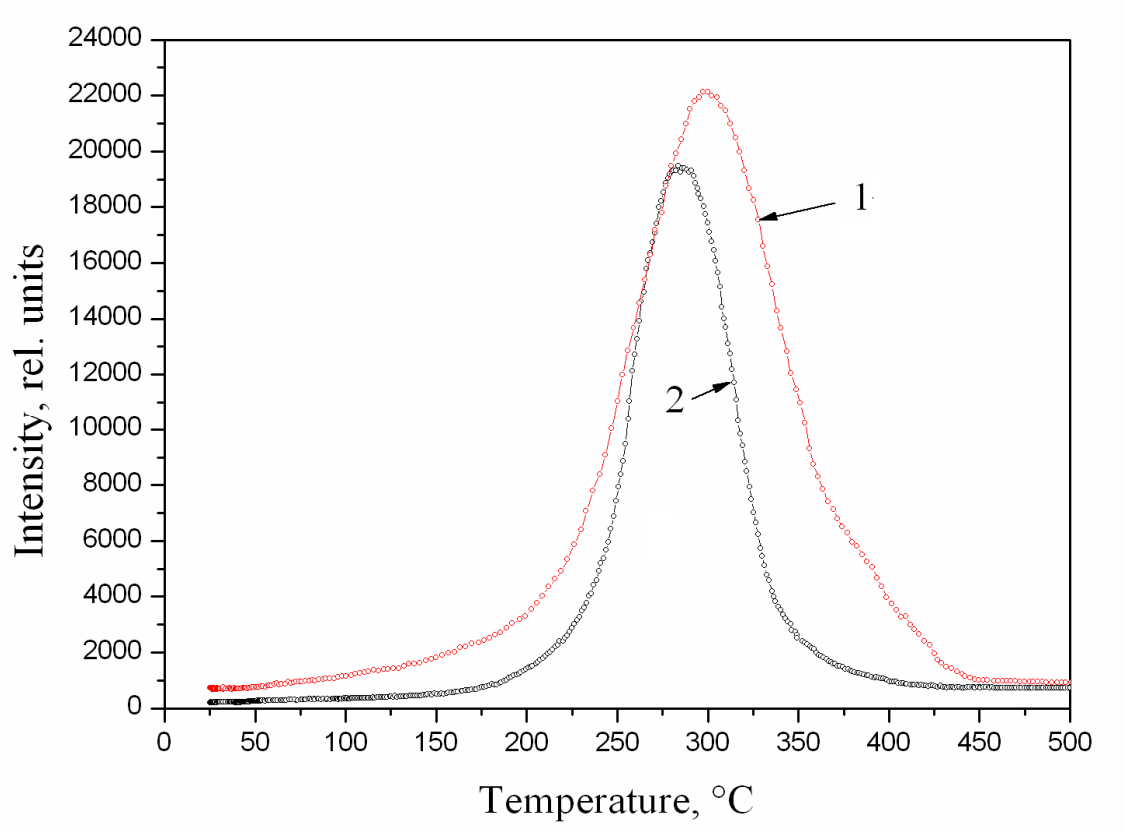

Fig. 5 Temperature dependence of the intensity of hydrogen evolution: 1 – $Ti_{19.8}Zr_{34.8}Mn_{43.3}V_{2.1}$, 2 – $Ti_{32.1}Zr_{18.9}Mn_{42.0}V_{7.0}$.

The characteristics of hydrogen sorption of alloys in the Ti–Zr–Mn system were improved by optimizing the titanium to zirconium ratio in the composition of the Laves phase, decreasing the lower concentration boundary of the intermetallic through alloying with vanadium, and the presence of a *bcc* solid solution. The sorption capacity of the Ti–Zr–Mn–V alloys was increased, the kinetic parameters of the hydrogen sorption and desorption processes were improved, and near one hundred percent reversibility was reached.

References

[1] B.P. Tarasov, M.V. Lototskii, V.A. Yartys', *Russ. J. Gen. Chem.* 77 (2007) 694-711.

[2] S. Samboshi, N. Masahashi, S. Hanada, *J. Alloys Compd*. 352 (2003) 210-217.

[3] Taizhong Huang, Zhu Wu, Yu Xuebin, Jinzhou Chen, Baojia Xia, Tiesheng Huang, Naixin Xu, *Intermetallics* 12 (2004) 91-96.

[4] Ming Au, F. Pourarian, S.G. Sankar, W.E. Wallace, Lian Zhang, *Mater. Sci. Eng. B* 33 (1995) 53-57.

[5] Bin-Hong Liu, Dong-Myung Kim, Ki-Young Lee, Jai-Young Lee, *J. Alloys Compd*. 240 (1996) 214-218.

[6] J.L. Bobet, B. Chevalier, B. Darriet, *Intermetallics* 8 (2000) 359-363.

[7] X.Y. Song, Y. Chen, Z. Zhang, Y.Q. Lei, X.B. Zhang, Q.D. Wang, *Int. J. Hydrogen Energy* 25 (2000) 649-656.

[8] Jeong-Gun Park, Hwan-Young Jang, Sang-Cheol Han, P.S. Lee, Jai-Young Lee, *Mater. Sci. Eng. A* 329-331 (2002) 351-355.

[9] V.G. Ivanchenko, V.A. Dekhtyarenko, T.V. Pryadko, *Powder Metall. Met. Ceram.* 52 (2013) 340-344.

[10] Yunlong Zhang, Jinshan Li, Tiebang Zhang, Tiandong Wu, Hongchao Kou, Xiangyi Xue, *J. Alloys Compd.* 694 (2017) 300-308.

[11] V.N. Verbetsky, S.V. Mitrokhin, *Materialovedenie* (Materials Sciences) (1) (2009) 48-59 (in Russian).

[12] V.A. Dekhtyarenko, *Metallofiz. Noveishie Tekhnol.* (Metal Physics and Advanced Technologies) 37 (2015) 683-685 (in Russian).

[13] S.V. Mitrokhin, *J. Alloys Compd*. 404-406 (2005) 384-387.

[14] S.V. Mitrokhin, T.N. Smirnova, V.A. Somenkov, V.P. Glazkov, V.N. Verbetsky, *J. Alloys Compd.* 356-357 (2003) 80-83.

[15] M. Kazemipour, H. Salimijazi, A. Saidi, A. Saatchi, A.A. Arjmand, *Int. J. Hydrogen Energy* 39 (2014) 12784-12788.

[16] L. Pickering, J. Li, D. Reed, A.I. Bevan, D. Book, *J. Alloys Compd.* 580 (2013) 233-237.

[17] Taizhong Huang, Zhu Wu, Guoxin Sun, Naixin Xu, *Intermetallics* 15 (2007) 593-598.

[18] V. Ivanchenko, in: G. Effenberg, S. Ilyenko (Eds.), Landolt-Börnstein, New Series, Group IV, Vol. 11, *Ternary Alloy Systems, Subvolume C, Non-Ferrous Systems*, Part 3, Springer-Verlag, Berlin-Heidelberg, 2007, pp. 475-485.

[19] V.A. Dekhtyarenko, *Metalozn. Obrob. Met.* (Metal Science and Treatment of Metals) (3) (2011) 48-51 (in Ukrainian).

[20] G.F. Kobzenko, A.A. Shkola, *Zavod. Lab.* (Industrial Laboratory) 56 (1990) 41-45 (in Russian).

[21] O.M. Ivasishin, V.T. Cherepin, V.N. Kolesnik, M.M. Gumenyuk, *Prib. Tekh. Eksp*. (Instruments and Experimental Techniques) (3) (2010) 147-151 (in Russian).